

Reactivity of a Cationic Alkyl Amino-Functionalized Cyclopentadienyl Aluminum Compound with Olefins: NMR Observation and Computational Investigation of the Single Propene Insertion Product into an Al–C Bond

Daniela Pappalardo,^{*,†} Claudio Pellecchia,[‡] Giuseppe Milano,[‡] and Massimo Mella^{*,§}

Dipartimento di Studi Geologici ed Ambientali, Università del Sannio, Via dei Mulini 59/A, I-82100, Benevento, Italy, Dipartimento di Chimica, Università di Salerno, Via Ponte don Melillo, I-84084, Fisciano (SA), Italy, and School of Chemistry, Cardiff University, Main Building, Park Place, Cardiff CF10 3AT, U.K.

Received October 15, 2008

In this study the reactivity of the compound dimethyl [2-(*N,N*-dimethylethylen)cyclopentadienyl]Al(III) toward ionizing species and the subsequent reactivity toward ethylene and propene have been explored. Reactions were studied via NMR tube experiments. Upon methyl abstraction by the Lewis acid B(C₆F₅)₃, the amine donor on the ligand side arm coordinates to aluminum, stabilizing the resulting cationic species versus secondary reactions. The obtained cationic species was able to polymerize ethylene, albeit with low activity. Reaction with propene resulted in the selective 1,2-insertion of one propene molecule into an Al–C bond of the Al–Cp moiety. Density functional and *ab initio* calculations were used to characterize the energy landscape of the insertion into the Al–Cp bond for both ethylene and propene. The computational results suggest this reaction to be more facile than the insertion into the Al–Me bond.

Introduction

Oligomerization and polymerization of ethylene and olefins are among the most important homogeneous catalytic processes. Since the discovery by Ziegler of the Aufbau reaction, aluminum alkyls have long been known as ethylene oligomerization catalysts¹ and widely used as “cocatalysts” or “scavengers” in Ziegler–Natta olefin polymerization catalysis.² On the contrary, olefin polymerization by means of transition metal-free aluminum-based catalytic species is a quite recent achievement. In 1992 Martin demonstrated that the simple bis(dichloroaluminum)-ethane and trialkylaluminum are able to produce polyethylene of high molecular weight in considerably mild conditions.³ In the past decade several examples have been described in the literature concerning olefin polymerization at aluminum, although with low activity. Following the reports of Jordan on mono- and bis(amidinate) complexes of aluminum,⁴ a few related dialkyl aluminum derivatives carrying chelating monoanionic ligands, such as aminotroponimine,⁵ bis(imino)pyridine,⁶

salicylaldimine,⁷ 2-anilinothione,⁸ and, more recently, a bis-(iminophosphorano)methandiide aluminum complex, based on a spirocyclic carbon center subtended by two AlMe₂ units,⁹ have also been shown to polymerize ethylene. Activation of these compounds was usually achieved by the ionizing agents traditionally used in homogeneous Ziegler–Natta catalysis (i.e., B(C₆F₅)₃ or [(C₆H₅)₃C][B(C₆F₅)₄]). Very interestingly, Sen et al. reported that simple aluminum alkyls, after reaction with ionizing agents, catalyze the polymerization not only of ethylene but also of propene,¹⁰ while recently simple aluminum alkyls in the presence of chloro activators were shown to promote ethylene polymerization in mild conditions with higher activity.¹¹

The nature of the active species involved in the ethylene polymerization with aluminum-based systems has been investigated; although cationic alkyl complexes have been isolated and characterized, it is still unclear if they are directly responsible for the catalytic activity. Monitoring the reaction of perdeuterio-ethylene with an aminotroponimine aluminum complex, Jordan excluded that intact cationic species are the active ethylene polymerization catalysts, while the main reaction is a β -H transfer to generate the corresponding cationic

* Corresponding authors. E-mail: pappalardo@unisannio.it; MellaM@cardiff.ac.uk.

[†] Università del Sannio.

[‡] Università di Salerno.

[§] Cardiff University.

(1) Ziegler, K.; Gellert, H.-G.; Zosel, K.; Holzkamp, E.; Schneider, J.; Söll, M.; Kroll, W.-R. *Justus Liebigs Ann. Chem.* **1960**, 629, 121–166.

(2) For leading references see: (a) Britzinger, H. H.; Fischer, D.; Mullhaupt, R.; Rieger, B.; Waymouth, R. M. *Angew. Chem., Int. Ed. Engl.* **1995**, 34, 1143. (b) Kaminsky, W.; Arndt, M. *Adv. Polym. Sci.* **1997**, 127, 143.

(3) Martin, H.; Bretinger, H. *Makromol. Chem.* **1992**, 193, 1283–1288.

(4) (a) Coles, M. P.; Swenson, D. C.; Jordan, R. F. *Organometallics* **1997**, 16, 5183–5194. (b) Coles, M. P.; Jordan, R. F. *J. Am. Chem. Soc.* **1997**, 119, 8125–8126. (c) Duchateau, R.; Meetsma, A.; Teuben, J. H. *Chem. Commun.* **1996**, 22, 3–224.

(5) (a) Ihara, E.; Young, V. G., Jr.; Jordan, R. F. *J. Am. Chem. Soc.* **1998**, 120, 8277–8278. (b) Korolev, A. V.; Ihara, E.; Guzei, I. A.; Young, V. G., Jr.; Jordan, R. F. *J. Am. Chem. Soc.* **2001**, 123, 8291–8309.

(6) Bruce, M.; Gibson, V. C.; Redshaw, C.; Solan, G. A.; White, A. J. P.; Williams, D. J. *Chem. Commun.* **1998**, 2523–2524.

(7) (a) Cameron, P. A.; Gibson, V. C.; Redshaw, C.; Segal, J. A.; Bruce, M. D.; White, A. J. P.; Williams, D. J. *Chem. Commun.* **1999**, 1883–1884. (b) Cameron, P. A.; Gibson, V. C.; Redshaw, C.; Segal, J. A.; White, A. J. P.; Williams, D. J. *J. Chem. Soc., Dalton Trans.* **2002**, 415–422. (c) Pappalardo, D.; Tedesco, C.; Pellecchia, C. *Eur. J. Inorg. Chem.* **2002**, 621–628.

(8) Pappalardo, D.; Mazzeo, M.; Montefusco, P.; Tedesco, C.; Pellecchia, C. *Eur. J. Inorg. Chem.* **2004**, 1292.

(9) Cavell, R. G.; Aparna, K.; Kamalesh Babu, R. P.; Wang, Q. *J. Mol. Catal. A: Chem.* **2002**, 189, 137–143.

(10) Kim, J. S.; Wojcieński, L. M., II; Liu, S.; Sworen, J. C.; Sen, A. *J. Am. Chem. Soc.* **2000**, 122, 5668–5669.

(11) Shaver, M. P.; Annan, L. E. N.; Gibson, V. C. *Organometallics* **2007**, 26, 2252–2257.

aluminum hydride.^{5a} According to a theoretical study on ethylene polymerization at aluminum centers, mononuclear aluminum species are unlikely to produce polymers, because chain transfer is much faster than propagation.¹² Therefore, the observed polymerization activity could be due to minor unidentified species produced *in situ*, and probably more complex structures have to be considered.

We noted that there has been little investigation into the reactivity with olefins of aluminum(III) compounds bearing cyclopentadienyl ligands,¹³ which instead were widely used for olefin polymerization catalysts.² Moreover, although cationic species represent potential candidates for catalysis due to the increased Lewis acidity,¹⁴ cationic aluminum species are quite unstable, and very often they undergo ligand scrambling reactions with the anion.¹⁵ The stability of the cationic species could be strongly improved by the presence of a Lewis base in the solvent medium¹⁶ or, even better, in the ligand itself.^{7a,b} Cyclopentadienyl ligands with tethered donor units have been largely used in the preparation of several compounds of s-, p-, d-, and f-block elements.¹⁷ In particular, cyclopentadienyl compounds with a dialkylaminoalkyl side chain have also been employed in transition metal olefin polymerization catalytic systems.^{17a,18} In this study we have explored the reactivity of dimethyl [2-(*N,N*-dimethylethylene)cyclopentadienyl]Al(III)¹⁹ toward ionizing species and the subsequent reactivity toward ethylene and propene. Monitoring the reaction of the obtained cationic species with propene allowed the observation of an unprecedented propene insertion product into an Al–C bond. The energy landscape of this reaction channel was also investigated by means of electronic structure calculations in the gas phase and shown to proceed through a low-lying transition state.

Results and Discussion

Experimental Results. Dimethyl [2-(*N,N*-dimethylethylene)cyclopentadienyl]Al(III) (**1**), synthesized according to the

literature,¹⁹ was allowed to react with 1 equiv of B(C₆F₅)₃²⁰ to give the cationic species [C₅H₅(CH₂CH₂NMe₂)AlMe]⁺–[MeB(C₆F₅)₃][–] (**2**). The reaction was studied via NMR in C₆D₅Cl solution at 25 °C (Figure 1a). Diagnostic resonances in the ¹H NMR spectrum of **2** are a singlet at –1.07 ppm attributable to the AlMe (3 H) and a singlet at +1.07 ppm (3 H) attributable to the “free” anion MeB(C₆F₅)₃[–].²⁰ Consistently, in the ¹³C NMR spectrum, a signal at –16.3 ppm attributable to AlMe and a signal at 10.1 ppm attributable to MeB(C₆F₅)₃[–] appear. In addition, the ligand resonances are shifted to higher field in comparison with those of the neutral starting compound. Concerning the cyclopentadienyl ligand, the presence of two singlets (6.15 and 5.79 ppm, 2 H each) in the ¹H NMR spectrum and of three signals (129.2, 121.3, and 96.5 ppm) in the ¹³C NMR spectrum is compatible with a “windscreen-wiper” fast haptotropic rearrangement process, already observed in analogous neutral compounds (Scheme 1).^{17c,19} Lower temperature ¹H NMR experiments performed in CD₂Cl₂ resulted in more complex spectra, with new signals in the Cp regions and two broad singlet at –1.09 and –1.78 ppm attributable to AlMe hydrogen atoms; the ¹³C NMR spectrum, registered at –60 °C, displayed five signals (130.1, 128.0, 124.7, 116.1, 111.6 ppm). These data indicate that at lower temperature the “windscreen-wiper” fluxional behavior is frozen out. It is worth noting that such a cationic species is stable for days in C₆D₅Cl solution at room temperature. On the contrary, the analogous reaction of CpAlMe₂ and B(C₆F₅)₃ did not result in stable or observable cationic species. Probably in our case the extra donor –NMe₂ unit could stabilize the cation against side reactions such as ligand redistribution.¹⁵

The reactivity of the cationic species **2** toward olefins was explored: compound **1**, when activated with 1 equiv of B(C₆F₅)₃, polymerized ethylene (1 atm) to solid polyethylene albeit with low activity (80 g (PE) mol^{–1} h^{–1} atm^{–1}), while, in the same conditions, it was inactive in the propene polymerization.

Interesting results were derived from the study of the reactivity of the cationic species **2** toward olefins by NMR tube reactions. To a solution of compound **2** in C₆D₅Cl was added propylene, and the reaction was monitored via ¹H NMR (Figure 1b,c). New resonances appeared just after a few minutes from the injection of propylene. After 2 h their intensities were in 1:2 ratio with respect to the original cationic aluminum species **2**. These resonances were attributed to a new organometallic cationic aluminum species (**3**), arising from the insertion of propylene into an Al–C bond of **2** (Scheme 2). Unexpectedly, the propylene does not insert into the Al–Me bond, but into the Al–Cp moiety of **2**. Density functional and *ab initio* calculations (*vide ultra*) were used to characterize the energy landscape of the reaction for both ethylene and propene and predicted a barrier of at least 23.4 kcal/mol for the insertion of the ethylene into the Al–Me bond, while the insertion into the Al–Cp bond presented very low barriers (4.3–4.8 kcal/mol). The structure of **3** was completely elucidated by the use of ¹H and ¹³C, mono- and bidimensional NMR experiments, including DEPT, COSY, and direct and long-range ¹H–¹³C correlation (Tables 1, 2, and 3), disclosing interesting features. First, the anion MeB(C₆F₅)₃[–] is not involved in the reaction, neither does it interact with the new cationic species. In the ¹H NMR spectrum the intensity of the singlet at +1.07 ppm (3 H, MeB(C₆F₅)₃[–]) remains constant. Consistently, the ¹⁹F NMR data

(12) (a) Talarico, G.; Budzelaar, P. H. M. *Organometallics* **2000**, *19*, 5691–5695. (b) Talarico, G.; Busico, V.; Budzelaar, P. H. M. *Organometallics* **2001**, *20*, 4721–4726. (c) Talarico, G.; Budzelaar, P. H. M. *Organometallics* **2002**, *21*, 34–38.

(13) (a) Shapiro, P. J. *Coord. Chem. Rev.* **1999**, *189*, 1–17. (b) Bochmann, M.; Dawson, D. M. *Angew. Chem., Int. Ed.* **1996**, *35*, 2226. (c) Burns, C. T.; Shapiro, P. J.; Budzelaar, P. H. M.; Willett, R.; Vij, A. *Organometallics* **2000**, *19*, 3361. (d) Lee, S.-J.; Shapiro, P. J.; Twamley, B. *Organometallics* **2006**, *25*, 5582–5588.

(14) For reviews on group 13 cationic compounds, see: (a) Atwood, D. A. *Coord. Chem. Rev.* **1998**, *176*, 407–430. (b) Atwood, D. A.; Dagorne, S. *Chem. Rev.* **2008**, *108* (10), 4037–4071.

(15) (a) The reaction between AlR₃ and B(C₆F₅)₃ was described in a patent application as a convenient approach to the synthesis of Al(C₆F₅)₃: Biagini, P.; Lugli, G.; Abis, L.; Andreussi, P. (Enichem Elastomeri S.r.l.) Eur. Patent Appl. EP 0 694 548 A1, 1996, pp 1–9. (b) Qian, B.; Ward, D. L.; Milton, R. S., III *Organometallics* **1998**, *17*, 3070–3076. (c) Bochmann, M.; Sarfield, M. J. *Organometallics* **1998**, *17*, 5908–5912.

(16) (a) Jegier, J. A.; Atwood, D. A. *Inorg. Chem.* **1997**, *36*, 2034–2039. (b) Klosin, G.; Roof, R. G.; Chen, E. Y.-X.; Abboud, K. A. *Organometallics* **2000**, *19*, 4684–4686.

(17) (a) Jutzi, P.; Redeker, T. *Eur. J. Inorg. Chem.* **1998**, 663–674. (b) Müller, C.; Vos, D.; Jutzi, P. *J. Organomet. Chem.* **2000**, *600*, 127–143. (c) Bensiak, S.; Bangel, M.; Neumann, B.; Stammer, H.-G.; Jutzi, P. *Organometallics* **2000**, *19*, 1292–1298.

(18) (a) Flores, J. C.; Chien, J. C. W.; Rausch, M. D. *Organometallics* **1994**, *13*, 4140–4142. (b) Emrich, R.; Heinemann, O.; Jolly, P. W.; Krüger, C.; Verhovnik, G. P. *J. Organometallics* **1997**, *16*, 1511–1513. (c) Bradley, S.; Camm, K. D.; Furtado, S. J.; Gott, A. L.; McGowan, P. C.; Podesta, T. J.; Thornton-Pett, M. *Organometallics* **2002**, *21*, 3443–3453.

(19) Jutzi, P.; Dahlhaus, J.; Bangel, M. *J. Organomet. Chem.* **1993**, *460*, C13–C15.

(20) (a) Massey, A. G.; Park, A. J. *J. Organomet. Chem.* **1964**, *2*, 245–250. (b) Yang, X.; Stern, C. L.; Marks, T. J. *J. Am. Chem. Soc.* **1991**, *113*, 3623–3625. (c) Yang, X.; Stern, C. L.; Marks, T. J. *J. Am. Chem. Soc.* **1994**, *116*, 10015–10031.

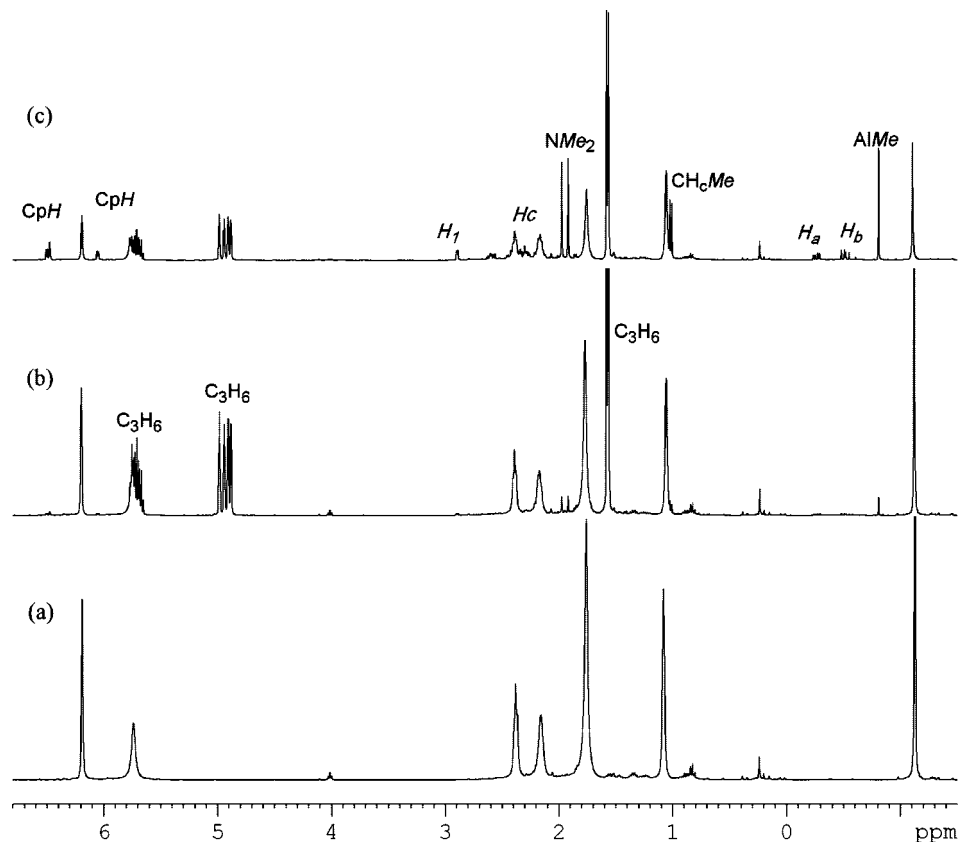
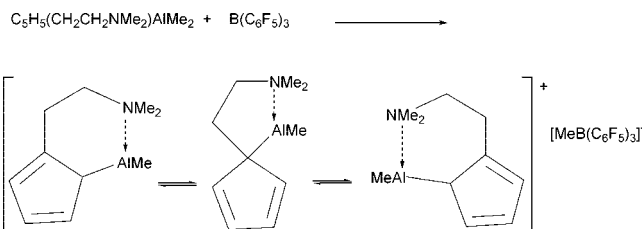
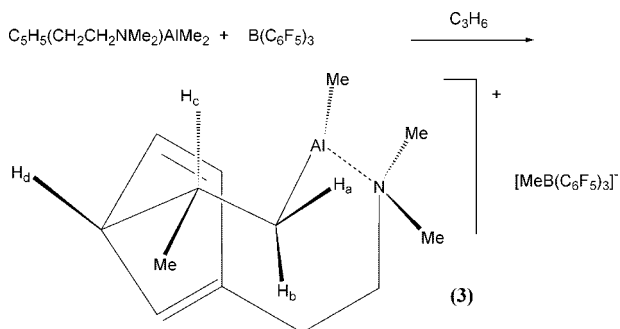


Figure 1. (a) ^1H NMR spectrum ($\text{C}_6\text{D}_5\text{Cl}$, 25°C) of $[\text{C}_5\text{H}_5(\text{CH}_2\text{CH}_2\text{NMe}_2)\text{AlMe}]^+[\text{MeB}(\text{C}_6\text{F}_5)_3]^-$ (**2**). (b, c) ^1H NMR spectra ($\text{C}_6\text{D}_5\text{Cl}$, 25°C) monitoring the reaction of **2** 5 min and 2 h, respectively, after the addition of propene.

Scheme 1



Scheme 2



are as expected for symmetric methyl-borate anions, showing no evidence of methyl or fluorine interactions with the cationic center.

In the ^1H NMR spectrum a characteristic resonance of the new species **3** is the singlet at -0.81 ppm (3 H), accounting for the Al-Me protons. In the ^{13}C NMR spectrum the corresponding carbon displays a resonance at -11.4 ppm. In the ^1H NMR spectrum diagnostic resonances for the propene insertion are the two doublets of doublets at -0.25 and -0.55 ppm, relative to the diastereotopic geminal hydrogen atoms (H_a and

Table 1. ^1H NMR ($\text{C}_6\text{D}_5\text{Cl}$, 25°C) Data for the Species **3**^a

δ (^1H)	assgnt
-0.81 (3 H, s)	AlMe
-0.55 (1 H, dd, $^2J = 15.0$, $^3J = 6.8$, $^4J = 1.5$)	Al-CHaHb-
-0.25 (1 H, dd, $^2J = 15.0$, $^3J = 1$)	Al-CHaHb-
1.01 (3 H, d, $^3J = 6.6$)	CHaHb-CHcMe
1.07 (3 H, s)	$[\text{MeB}(\text{C}_6\text{F}_5)_3]^-$
1.92 (3 H, s)	$\text{CH}_2\text{CH}_2\text{NMeMe}'$
1.97 (3 H, s)	$\text{CH}_2\text{CH}_2\text{NMeMe}'$
2.18 (2 H, m)	$\text{CH}_2\text{CH}_2\text{NMeMe}'$
2.30 (2 H, m)	$\text{CH}_2\text{CH}_2\text{NMeMe}'$
2.42 (1 H, m)	CHaHb-CHcMe
2.90 (1 H, m)	Hd (C ₅ ring)
6.05 (1 H, d, $^3J = 5.6$)	H (C ₅ ring)
6.47 (1 H, s, br)	H (C ₅ ring)
6.50 (1 H, d, $^3J = 5.6$)	H (C ₅ ring)

^a All chemical shifts are in ppm and J values in Hz.

H_b) bound to the carbon in α -position with respect to Al. H-H COSY analysis confirms that both hydrogen atoms H_a and H_b correlate with the same CH hydrogen (H_c , 2.18 ppm); likewise, this H_c hydrogen is coupled with a methyl group, appearing as a doublet at 1.01 ppm (Figure 2). A HMBC (heteronuclear multiple bond correlation) ^1H - ^{13}C 2D NMR experiment established unambiguously the structure, through observation of the C-H correlation between the β -carbon atom of the propene inserted unit (Al-CH₂-CHMe, 35.6 ppm) and the hydrogen bound to the sp^3 -hybridized C5-ring carbon atom (H_d , 2.90 ppm). In addition, in the ^1H NMR spectrum a long-range coupling constant ($^4J = 1.5$ Hz) between H_a and the hydrogen atom bound to the sp^3 carbon atom of the C5 ring (H_d) was observed, consistent with a stereorigid "W" conformation of the four bonds between these two hydrogen atoms.

The insertion of propylene therefore was highly regiospecific, affording exclusively the 1,2-insertion product. The structure

Table 2. ^{13}C NMR ($\text{C}_6\text{D}_5\text{Cl}$, 25 °C) Data for the Species **3**^a

δ (^{13}C)	assgnt
–11.4	AlMe
7.9	Al–CH ₂ –CHMe
11.2	BMe
25.0	Al–CH ₂ –CHMe
25.5	(C ₅ H ₄)CH ₂ CH ₂ NMeMe'
35.6	Al–CH ₂ –CHMe
44.4	(C ₅ H ₄)CH ₂ CH ₂ NMeMe'
44.7	(C ₅ H ₄)CH ₂ CH ₂ NMeMe'
58.9	(C ₅ H ₄)CH ₂ CH ₂ NMeMe'
68.0	CHd (C ₅ ring)
129.6	CH (C ₅ ring)
138.0	CH (C ₅ ring)
149.5	CH (C ₅ ring)
157.0	C (quaternary; C ₅ ring)

^a All chemical shifts are in ppm.

of the product was identified by careful consideration of the coupling constants to H_a in the ^1H NMR spectrum. In fact, the signal at –0.55 ppm appears as a doublet of doublets, with further fine structure due to the long-range coupling. The geminal ($^2J(\text{H}_a\text{--H}_b) = 15.0$ Hz) and the vicinal ($^3J(\text{H}_a\text{--H}_c) = 6.8$ Hz) coupling constants reveal significantly different values depending on the small H_a–C–C–H_c dihedral angle. The molecule seems to be locked in a pseudo-metallacycle, where the methyl group originating from propene insertion occupies preferentially an equatorial position. The nitrogen atom should be strongly coordinated to the Al, as evidenced by the appearance of two singlets for the NMe₂ groups both in the ^1H (1.92 and 1.97 ppm) and ^{13}C (44.4 and 44.7 ppm) NMR spectra. Concerning the C₅ ring, in the ^{13}C NMR spectrum five distinct resonances are observed (68.0, 129.6, 138.0, 149.0, 157.0), clearly indicating a locked position of the two C–C double bonds. The low-field ^1H NMR spectrum pattern, in fact, is the one expected for a 1,3-disubstituted cyclopentadiene ring.

Consistently, density functional and *ab initio* calculations (*vide ultra*) also indicated a better stability and a lower transition state energy barrier for the regioisomers deriving from the 1,2-insertion, which could also be explained in terms of Mulliken population of the olefin sp² carbon atoms. Moreover, as a further support to the whole structure, the calculated proton chemical shifts (*vide ultra*) are in good agreement with the experimental results.

In order to force the reaction to completion, the solution was warmed at higher temperature (i.e., 50 °C), but as a result only decomposition products were obtained. Removal of propene did not cause any deinsertion reaction. Consistently with this result, the computed barrier to the deinsertion reaction was high (see Table 4). On the contrary, when more propene was added to replace the consumed one, the reaction was forced to completion; at room temperature in a 30 h reaction period, **3** became the prevalent species (in 1.5:1 molar ratio with respect to **2**). Attempts to isolate the species **3** as analytically pure material, performed on larger scale reaction, were unsuccessful: the reactions gave no clean products, probably due to the extreme air sensitivity of the cationic aluminum species.

The reactivity of compound **2** toward ethylene was studied in analogous experiments. Monitoring the reaction of compound **2** with ethylene (3 equiv) in $\text{C}_6\text{D}_5\text{Cl}$ solution at 23 °C showed that the amount of **2** and ethylene gradually decreased in 1:1 molar ratio. After 6 h, the concentrations of **2** and of ethylene were respectively 55% and 80% of the initial ones. Conversely new resonances, attributable to the Al–Cp ethylene insertion product **4**, analogous to **3**, appeared. Characteristic resonances were the singlet at –0.85 ppm, attributable to the AlMe⁺ of the

new cationic aluminum species, and two doublets of doublets at –0.26 and –0.46 ppm, attributable to the diastereotopic geminal hydrogen atoms (H_a and H_b) bound to the carbon in α -position with respect to Al.

Consistently with the above structure, compound **3** does not further react with propene; formation of polypropene was not detected even at a prolonged reaction time (24 h). Following a reviewer's suggestion, in another experiment, **3** was generated *in situ*, and then some ethylene was further added. The reaction was monitored by ^1H NMR. Interestingly, after a 4 h period, the concentration of **3** remained unchanged. On the contrary, the concentration of **2** decreased, as well as the concentration of ethylene, and as already observed above formation of **4** was detected. In conclusion while at the moment the identification of the real catalytic species responsible for the ethylene polymerization is still elusive, the performed NMR experiments clearly indicate a preference for olefin insertion into the Al–Cp bond.

Computational Results. The final structure of the stationary points on the B3LYP/6-311+G(d,p) potential energy surface for the ethylene insertions (i.e., the cation **2**, its complex with ethylene (**CE**), the transition state (**TS**) describing the insertion of ethylene into the Al–Cp bond (**TS-E1**), the TS for the insertion of ethylene into the Al–Me bond (**TS-E2**), and the end product (**PE1**) of the insertion into the Al–Cp bond) is shown in Figure 3. Figure 4 shows the equivalent structures for the propene insertion into the Al–Cp bond. Table 4 provides the relative energetics of **TS-E1**, **TS-E2**, and **PE1** with respect to the ethylene–cation (**CE**) complex and of the transition states (**TS-P1–4**) and products (**PP1–4**) with respect to the related complexes (**CP1–4**) for the propene insertion.

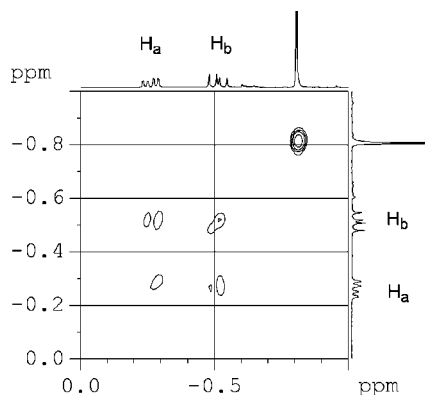
From Figure 3, we notice that the geometries of **CE**, **TS-E1**, and **PE1** present a relatively short Al–Cp distance, suggesting the presence of an interaction between Al and the Cp ring during all reaction stages. The structures of **CE** and **TS-E1** seem to suggest Al features a η^1 -coordination with the Cp ring, whereas the proximity of Al to the ring in **PE1** is likely due to the polarization of the Cp ring by the positively charged metal ion. One also notices that the gas phase equilibrium structure of **2** has Al located over the electron-rich Cp ring, thus suggesting a η^5 -coordination with the latter. The low-temperature ^{13}C NMR spectrum for this species indicates an asymmetric chemical environment for the ring carbons. Theoretical ^{13}C NMR chemical shifts for **2** (129.7 ppm for C1, 101.4 ppm for C2, 125.4 ppm for C3, 123.2 ppm for C4, and 108.1 ppm for C5, as computed at the B3LYP/6-311+G(2d,2p) level) show, accordingly, a nonsymmetric pattern in agreement with the experimental data. A similar lack of symmetry is found also in the distances between Al and the carbon atoms in the Cp ring (2.165, 2.180, 2.314, 2.322, and 2.192 Å) and in the Al–C bond orders (0.2779, 0.3175, 0.2308, 0.2259, and 0.3095) computed using the natural bond order (NBO) approach. The difference in Al–C distances appears to be due to a weak strain in the structure induced by the specific conformation of the CH₂CH₂NMe₂ ligand obtained during geometry optimization, which should disappear upon increasing the system temperature thanks to a more fluxional behavior of the CH₂CH₂NMe₂ group. As for the Al–C bond orders, we notice that our data indicate the presence of a fractional bonding of Al with *all* the ring carbons, although a weak preference is present toward the substituted carbon in the ring and its two neighbors. In our view, this suggests Al to have either a η^3 - or η^5 -coordination with the Cp ring in **2**.

Despite the aforementioned similarity between experimental and theoretical ^{13}C NMR shift patterns and the fact that ring-

Table 3. Summary of the Long-Range Correlations Observed in the HMBC Spectrum ($\text{C}_6\text{D}_5\text{Cl}$, 25 °C) for the Species **3** ($\Delta = 100 \mu\text{s}$)^a

δ (^1H)	assgnt	δ (^{13}C)	assgnt
−0.55 (1 H, dd, $^2J = 15.0$, $^3J = 6.8$, $^4J = 1.5$)	Al-CHaHb-CHcMe	35.6	Al-CH ₂ -CHcMe
−0.25 (1 H, dd, $^2J = 15.0$, $^3J = 11$)	Al-CHaHb-CHcMe	25.0	Al-CH ₂ -CHcMe
1.01 (3 H, d, $^3J = 6.6$)	Al-CHaHb-CHcMe	35.6	Al-CH ₂ -CHcMe
		68.0	CHd C ₅ ring
		35.6	Al-CH ₂ -CHcMe
1.92 (3 H, s)	(C ₅ H ₄)CH ₂ CH ₂ NMeMe'	58.9	(C ₅ H ₄)CH ₂ CH ₂ NMeMe'
		44.4	(C ₅ H ₄)CH ₂ CH ₂ NMeMe'
1.97 (3 H, s)	(C ₅ H ₄)CH ₂ CH ₂ NMeMe'	58.9	(C ₅ H ₄)CH ₂ CH ₂ NMeMe'
		44.7	(C ₅ H ₄)CH ₂ CH ₂ NMeMe'
2.18 (2 H, m)	(C ₅ H ₄)CH ₂ CH ₂ NMeMe'	129.6	C ₅ ring
		58.9	(C ₅ H ₄)CH ₂ CH ₂ NMeMe'
		44.7	(C ₅ H ₄)CH ₂ CH ₂ NMeMe'
2.30 (2 H, m)	(C ₅ H ₄)CH ₂ CH ₂ NMeMe'	157.0	C ₅ ring
		58.9	(C ₅ H ₄)CH ₂ CH ₂ NMeMe'
2.42 (1 H, m)	Al-CHaHb-CHcMe	157.0	C ₅ ring
		138.0	C ₅ ring
		68.0	CHd C ₅ ring
2.90 (1 H, m)	Hd C ₅ ring	157.0	C ₅ ring
		138.0(w)	C ₅ ring
		129.6	C ₅ ring
		35.6	Al-CH ₂ -CHcMe
6.05 (1 H, d, $^3J = 5.6$)	H C ₅ ring	138.0	C ₅ ring
6.47 (1 H, s)	H C ₅ ring	157.0	C ₅ ring
		68.0	CHd C ₅ ring
6.50 (1 H, d, $^3J = 5.6$)	H C ₅ ring	129.6	C ₅ ring

^a All chemical shifts are in ppm and J values in Hz. Weaker correlations, corresponding to smaller coupling constants, are identified with "w".

**Figure 2.** Aliphatic region H–H COSY NMR spectrum ($\text{C}_6\text{D}_5\text{Cl}$, 25 °C) of the reaction of $[\text{C}_5\text{H}_5(\text{CH}_2\text{CH}_2\text{NMe}_2)\text{AlMe}]^+[\text{MeB}(\text{C}_6\text{F}_5)_3]^-$ (**2**) with propene.

coordinated cationic complexes between Al and dicarbollylamine ligands similar to **2** were previously characterized by X-ray crystallography, NMR spectroscopy, and DFT calculations, we feel that it would be a hazard to draw a definitive conclusion about the possible changes induced by temperature in the structure of **2**.²¹ This uncertainty is mostly due to the absence of explicit solvent molecules in our calculations, which may induce further distortions in the structure of **2** following coordination with the Al cation as found in the case of **CE**.

As for the energetics of the ethylene insertions, Table 4 indicates already at first glance a good agreement between the energy profile for the insertion into both the Al–Cp and Al–Me bonds provided by the two levels of theory. Overall, our theoretical results indicate the insertion into the Al–Cp bond to be more facile than the one into the Al–Me bond by roughly 19 kcal/mol, in good agreement with the experimental results that indicate the preferential formation of **3**.

In an attempt to interpret the driving force and mechanism (electrophilic attack of the activated olefin on the Cp ring or

Table 4. Energetics of Ethylene and Propene Insertion Processes into the Al–Cp and Al–Me Bonds

	relative energy ^a	
	B3LYP/6-311 +G(d,p)	MP2/6-211 +G(d,p)
Ethylene		
TS-E1 Al–Cp bond insertion	4.3	4.8
TS-E2 Al–Me bond insertion	23.4	24.2
product (PE1) Al–Cp bond insertion	−14.1	−18.3
TS-E1 Al–Cp bond deinsertion	18.3	23.1
Propene		
TS-PP1 Al–Cp bond insertion	7.6	4.6
TS-PP2 Al–Cp bond insertion	7.4	4.7
TS-PP3 Al–Cp bond insertion	16.5	9.4
TS-PP4 Al–Cp bond insertion	13.7	9.4
product (PP1) Al–Cp bond insertion	−6.4	−14.1
product (PP2) Al–Cp bond insertion	−8.0	−15.9
product (PP3) Al–Cp bond insertion	−3.3	−14.4
product (PP4) Al–Cp bond insertion	−4.1	−11.6
TS-PP1 Al–Cp bond deinsertion	13.9	18.6
TS-PP2 Al–Cp bond deinsertion	15.4	20.6
TS-PP3 Al–Cp bond deinsertion	19.8	23.8
TS-PP4 Al–Cp bond deinsertion	17.8	21.1

^a Energies (kcal/mol) computed using the complex between the cationic species and each olefin as reference.

vice versa) for the latter reaction, Mulliken atomic charges were computed for **CE**. Unfortunately, this method failed to provide a clear-cut suggestion, with the C atoms involved in the reaction in both ethylene and the Cp ring bearing negative partial charges. In fact, if one excludes the C atoms in positions 1 (+0.08) and 2 (−0.36) with respect to the ring substituent and in close proximity to the positive Al atom in **CE**, the remaining carbons in the Cp ring bear smaller negative charges (−0.20 on C3, −0.11 on C4, and −0.16 on C5) than the olefin ones (−0.36 on the carbon closer to the ring and −0.30 on the other). An inspection of the DFT molecular orbitals on **TS-E1** highlighted, however, the presence of an overlap between the unoccupied ethylene π^* and an occupied orbital of the Cp ring (TS/HOMO, Figure 5a). The latter interaction appears to be stabilizing the HOMO orbital (−10.4 kcal/mol at the B3LYP/6-311+G(d,p) level) at the TS geometry with respect to the HOMO in the complex, which is highly localized on the ring. Roughly

(21) Lee, J.-D.; Kim, S.-K.; Kim, T.-J.; Han, W.-S.; Lee, Y.-J.; Yoo, D.-H.; Cheong, M.; Ko, J.; Kang, S. O. *J. Am. Chem. Soc.* **2008**, *130*, 9904–9917.

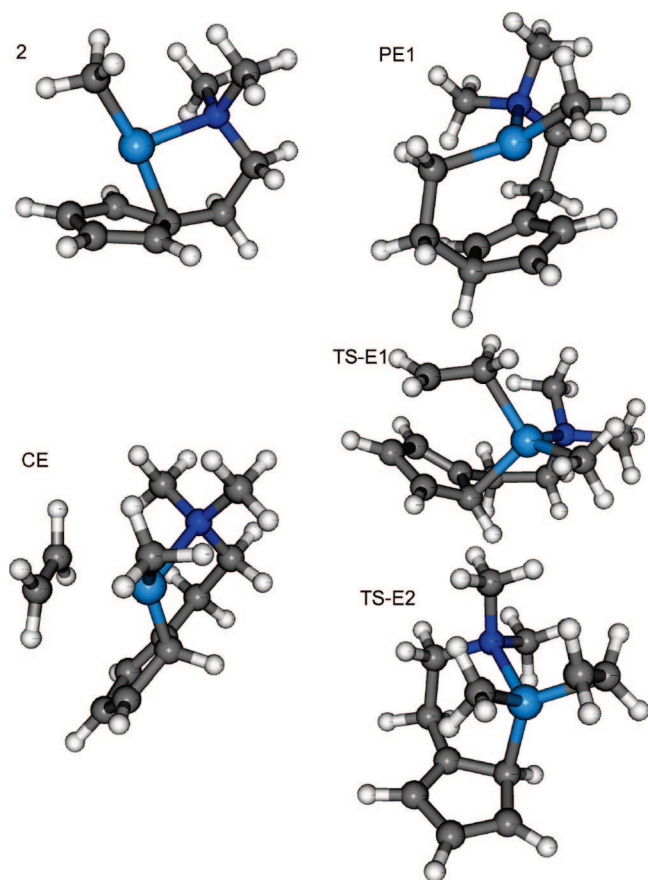


Figure 3. Optimized structures of the cationic species **2**, its complex with ethylene (**CE**), the transition state for the ethylene insertion into the Al–Cp (**TS-E1**) and Al–Me (**TS-E2**) bonds, and the product of the ethylene insertion into the Al–Cp bond (**PE1**).

speaking, this finding may be interpreted as indicating that the electron donation from the occupied Cp HOMO to the unoccupied ethylene π^* may be identified as largely responsible for lowering the barrier. In fact, the other high lying valence orbitals (HOMO-1–HOMO-3) describing the π -systems on both Cp and ethylene increase in energy at the TS geometry. In other words, the mechanism of the transformation appears to be mostly driven by the nucleophilic attack of the Cp ring onto ethylene despite the smaller Mulliken charges borne by the ring carbon atoms (also, *vide infra* for propene).

A similar conclusion is reached studying the regioselectivity of the propene insertion into the Cp–Al bond, on which we decided to focus given the substantially lower energy barrier found in the study with ethylene. Similarly to the latter case, the barriers separating the complexes from the insertion products are predicted to be low by both theoretical methods, with MP2 suggesting slightly lower barriers than DFT. From these results, however, it also appears that the formation of products having the methyl group of the propene closer to the ring (**PP1** and **PP2**) is more facile (roughly 4–6 kcal/mol depending on the theoretical method) than for the other two regioisomers (**PP3** and **PP4**). This finding is clearly in optimal agreement with the NMR characterization of the product, suggesting the formation of species with only a hydrogen close to the Cp ring. This result can be easily understood on the basis of our mechanistic suggestion surveying the coordination and Mulliken population of the olefin sp^2 carbon atoms in the complexes as shown for two representative complexes (**CP1** and **CP4**) in Figure 5b. Due to their geometry, both **CP1** and **CP2** present the almost neutral secondary carbon atom in the coordinated propene

($\text{CH}_2=\text{CHMe}$, +0.02) geometrically available for the nucleophilic attack by the Cp ring thanks to a preferential η^1 -coordination between Al and the unsubstituted CH_2 carbon atom. Conversely, the formation of **PP3** and **PP4** from **CP3** and **CP4** requires the olefin to shift closer to the Cp ring in order to facilitate the nucleophilic attack onto the negatively charged carbon (−0.51) in CH_2 , a displacement that should be expected to somewhat contribute to the increase in the energy barrier for the process. The larger negative charge and the structural requirement to form **PP3–4** also help in explaining the higher barrier that needs to be surmounted in forming **PP3** and **PP4** than in the case of **PE1**. As a final comment, it is also useful to mention that the reaction energy, computed as the difference between complex and product energies (Table 4), indicates a somewhat better stability for **PP1** and **PP2** than for **PP3** and **PP4** with respect to their parent complexes, thus suggesting that **PP1** and **PP2** should be preferentially found even in the case of an equilibrium process.

An additional support for the preferential formation of **3**, in either the **PP1** or **PP2** form, is provided by the computed chemical shifts²² of H_a , H_b , and H_c (Scheme 2) reported in Table 5 for the four possible regioisomers. As discussed in the Experimental Section, the signals of these three protons play a key role in elucidating the structure of **3**. Similarly, the theoretical results indicate a distinctively different pattern for the **PP1–2** and **PP3–4** pairs: whereas the former presents a single proton resonating around 3 ppm (lower field) and two protons absorbing around 0 ppm (higher field), the latter has two protons shifted to lower field and one at slightly higher field. Comparing with the chemical shifts reported in Table 1, it appears evident that only the chemical shifts of the **PP1–2** pair match the experimentally observed pattern of signals. As for the absolute accuracy of the computed NMR shifts, we point out that an offset of roughly 0.5 ppm between the experimental and theoretical data is a quite acceptable result²³ considering that possible effects due to solvation have not been taken into account in our model calculations. Due to this, a definitive discrimination between **PP1** and **PP2** based on a finer matching of chemical shifts would be inappropriate.

Conclusions

In this study, we have explored the reactivity of dimethyl [2-(*N,N*-dimethylethylene)cyclopentadienyl]Al(III) toward ionizing species and the subsequent reactivity toward ethylene and propene. After abstraction of the methyl group by the ionizing agent $\text{B}(\text{C}_6\text{F}_5)_3$, the amine function on the side arm coordinates to aluminum, stabilizing the resulting cationic species versus secondary reactions. The cyclopentadienyl ligand having a tethered amine unit offers a good balance of stability and reactivity. The obtained cationic species was able to polymerize ethylene, albeit with low activity. Quite surprisingly, conversely, reaction with propene resulted in the selective insertion of one propene molecule into an Al–C bond of the Al–Cp moiety. The energy landscape of both processes was explored by means of electronic structure methods, with results for the transition state barrier heights and proton chemical shifts strongly supporting the interpretation of the experimental results.

The carbalumination, i.e., the insertion of olefins into an Al–C bond, is a well-known reaction;²⁴ it is enough to mention

(22) McWeeny, R. *Phys. Rev.* **1962**, *126*, 1028.

(23) Helgaker, T.; Jaszunski, M.; Ruud, K. *Chem. Rev.* **1999**, *99*, 293.

(24) Eish J. J. In *Comprehensive Organometallic Chemistry II*; Abel, Stone, Wilkinson, Eds.; Pergamon: Exeter, 1995; Chapter 10: Aluminum, pp 464–467.

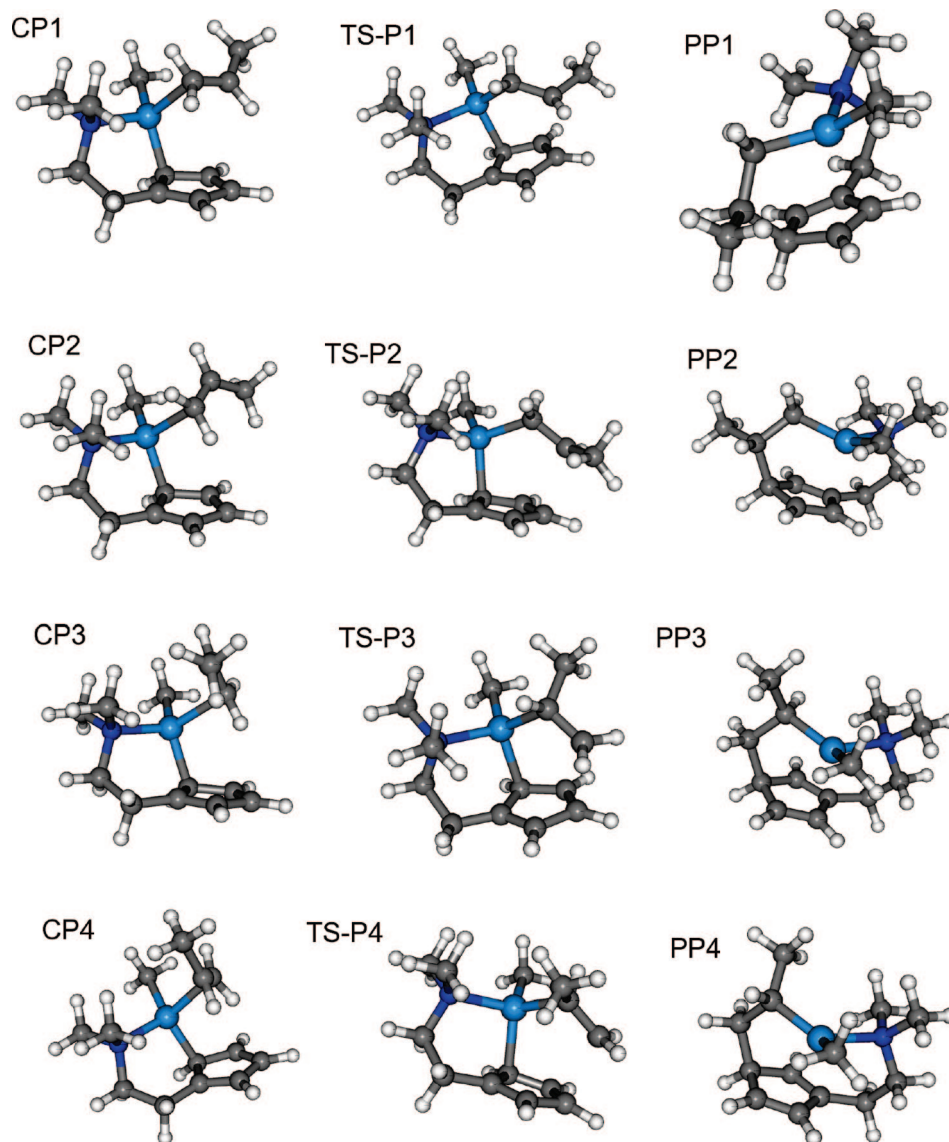


Figure 4. Optimized structure for the complexes between the cationic species **2** and propene (**CP1–4**), the transition states (**TS-P1–4**), and products (**PP1–4**) for the propene insertion into the Al–Cp bond.

that the insertion of ethene into Al–ethyl bonds is the basis of the original Aufbau reaction for the preparation of a mixture of α -alkenes or alcohols (C_4 – C_{30}).¹ Nevertheless, to our knowledge, direct observation of the reaction product deriving from the single insertion of propene into an Al–C bond has never been reported. Single olefin insertion products have been instead observed with some early transition metals and constituted models of intermediates for the insertion mechanism in Ziegler–Natta polymerization.²⁵ The observation that propene undergoes an insertion reaction into the Al–Cp moiety of the species **2** showed that this bond is more reactive than the Al–Me bond, which acts instead as a spectator ligand. It is worth nothing

that this behavior is the opposite of the one observed with the classical homogeneous transition metal-based catalytic systems for olefin polymerization, for which the metal–alkyl bond is the reactive one, while the cyclopentadiene acts as an “ancillary” ligand.² Actually, the present case has much in common with an earlier report by Jordan on the reversible cycloaddition reactions of ethylene and alkynes to cationic β -diketiminate aluminum complexes.²⁶ Density functional theory²⁷ was used to study the factors that influence these reactions and predicted barriers for the cycloaddition reactions significantly lower than those previous calculated for ethylene insertion in the Al–alkyl bonds of cationic aluminum alkyl complexes.¹²

Such results nicely agree with our present conclusions and further confirm the experimental observation that the cationic species **2** selectively inserts one propene molecule into an Al–C bond of the Al–Cp moiety rather than into the Al–methyl bond.

(25) (a) Pellecchia, C.; Grassi, A.; Zambelli, A. *J. Chem. Soc., Chem. Commun.* **1993**, 947–949. (b) Pellecchia, C.; Immirzi, A.; Grassi, A.; Zambelli, A. *J. Organomet. Chem.* **1994**, 479, C9–C11. (c) Pellecchia, C.; Grassi, A.; Zambelli, A. *Organometallics* **1994**, 13, 298–302. (d) Horton, A. D.; de With, J. *Organometallics* **1997**, 16, 5424–5436. (e) Gielen, E. C. G.; Dijkstra, T. W.; Berno, P.; Meetsma, A.; Hessen, B.; Teuben, J. H. *J. Organomet. Chem.* **1999**, 591, 88–95. (f) Corradi, M.; Jimenez Pindado, G.; Sarsfield, M. J.; Thornton-Pett, M.; Bochmann, M. *Organometallics* **2000**, 19, 1150–1159. (g) Shafir, A.; Arnold, J. *Organometallics* **2003**, 22, 567–575. (h) Anderson, L. L.; Schmidt, J. A. R.; Arnold, J.; Bergman, R. G. *Organometallics* **2006**, 25, 3394–3406.

(26) Radzewich, C. E.; Coles, M. P.; Jordan, R. F. *J. Am. Chem. Soc.* **1998**, 120, 9384–9385.

(27) Ariafard, A.; Lin, Z.; Jordan, R. F. *Organometallics* **2005**, 24, 5140–5146.

TS-HOMO E=-0.35968 hartree

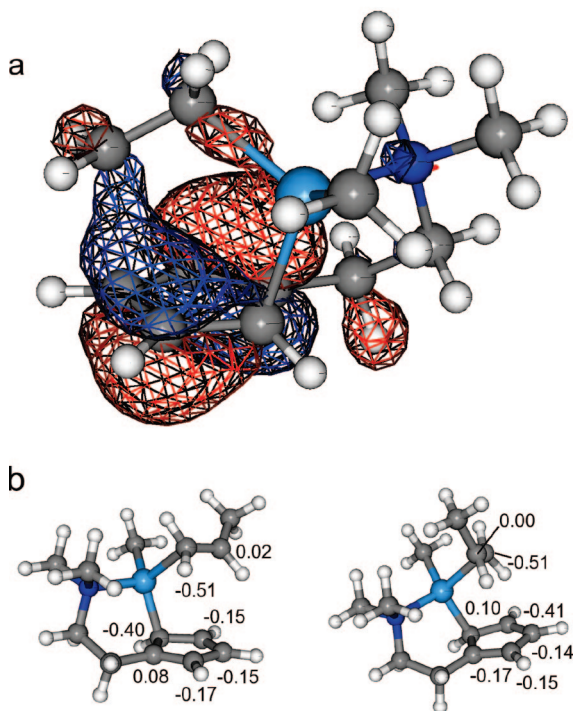


Figure 5. (a) Transition state HOMO molecular orbital at the B3LYP/6-311+(d,p) level (energies in hartree). (b) Mulliken charge population for complexes **CP1** and **CP4** at the B3LYP/6-21(d) level.

Table 5. ^1H Chemical Shifts Characterizing the Four Possible Products of the Propene Insertion into the Al–Cp Bond Computed at the B3LYP/6-311+G(2d,2p) Level

species	^1H δ (ppm) H_a , H_b , H_c
PP1	3.1098, 0.2855, -0.1894
PP2	2.9345, 0.3317, -0.4666
PP3	2.1623, 2.896, 0.4032
PP4	3.2951, 1.9425, 0.6886

Experimental Section

General Procedures. Manipulations of sensitive materials were carried out under a dry nitrogen atmosphere using Schlenk or glovebox techniques. ClC_6H_5 and ClC_6D_5 were dried over CaH_2 and distilled prior to use. Polymerization grade ethylene and propene (SON) were used without purification. The compounds dimethyl [2-(*N,N*-dimethylethylene)cyclopentadienyl]Al(III)¹⁹ and $\text{B}(\text{C}_6\text{F}_5)_3$ ²⁰ were synthesized according to literature procedures. NMR spectra were recorded on a Bruker Advance 400 MHz spectrometer (^1H , 400 MHz; ^{13}C , 100 MHz; ^{19}F 376 MHz); chemical shifts were referenced to the residual protio impurity of the deuterated solvent.

Ethylene Polymerization Tests. A typical polymerization test was carried out in a 100 mL glass flask charged under nitrogen with 12 mL of dry ClC_6H_5 and thermostatted at 23 °C. The inert gas was replaced by ethylene at 1 atm, then 0.05 mmol of dimethyl [2-(*N,N*-dimethylethylene)cyclopentadienyl]Al(III) and 0.05 mmol of $\text{B}(\text{C}_6\text{F}_5)_3$ (each dissolved in 1.0 mL of ClC_6H_5) were injected into the flask. The flask was fed with constant monomer pressure, and after 1 h the reaction was stopped by injecting methanol. The mixture was poured into acidified methanol, and the polymer was recovered by filtration, washed with fresh methanol, dried under vacuum, and analyzed by DSC and NMR (mp: 137 °C; ^{13}C NMR in $\text{C}_2\text{D}_2\text{Cl}_4$; 120 °C, δ in ppm from TMS: 30.00).

Generation of $[\text{C}_5\text{H}_5(\text{CH}_2\text{CH}_2\text{NMe}_2)\text{AlMe}]^+[\text{MeB}(\text{C}_6\text{F}_5)_3]^-$ (2**).** In a glovebox dimethyl [2-(*N,N*-dimethylethylene)cyclopentadienyl]Al(III) (13 mg, 0.065 mmol) was allowed to react with

$\text{B}(\text{C}_6\text{F}_5)_3$ (33 mg, 0.065 mmol) in 0.5 mL of $\text{C}_6\text{D}_5\text{Cl}$ at 20 °C. The solution was analyzed by NMR spectroscopy at room temperature. ^1H NMR (ClC_6D_5 , 293 K): δ -1.07 (s, 3H, Al-CH₃), 1.07 (s, 3H, B-CH₃), 1.69 (s, 6H, N-(CH₃)₂), 2.11 (t, 2H, Cp-CH₂), 2.35 (t, 2H, NCH₂), 5.79 (s, 2H, Cp-H), 6.15 (s, 2H, Cp-H). ^{13}C NMR (ClC_6D_5 , 293 K): δ -16.35 (Al-CH₃), 10.12 (B-CH₃), 25.25 (Cp-CH₂), 44.17 (N-(CH₃)₂), 59.30 (NCH₂), 96.55 (Cp-C_{2,5}), 116.94 (Cp-C_{3,4}), 129.22 (Cp-C₁). ^{19}F NMR (ClC_6D_5 , 293 K): δ -132.2 (d, 3J = 22 Hz), -164.9 (t, 3J = 21 Hz), -167.3 (t, 3J = 21 Hz).

Reaction of $[\text{C}_5\text{H}_5(\text{CH}_2\text{CH}_2\text{NMe}_2)\text{AlMe}]^+[\text{MeB}(\text{C}_6\text{F}_5)_3]^-$ (2**) with Ethylene.** In a J-Young NMR tube, dimethyl [2-(*N,N*-dimethylethylene)cyclopentadienyl]Al(III) (0.001 mmol) and $\text{B}(\text{C}_6\text{F}_5)_3$ (0.001 mmol) were dissolved in 0.7 mL of $\text{C}_6\text{D}_5\text{Cl}$ containing C_6H_6 (0.04 M) as internal standard and previously saturated with ethylene (3 equiv, measured by ^1H NMR) at 23 °C. The reaction was monitored via NMR spectroscopy at 23 °C. The NMR spectra showed that the amount of **2** and ethylene gradually decreased in a 1:1 molar ratio. After 3 h, the concentrations of **2** and of ethylene were respectively 70% and 89% of the initial ones, and after 6 h 55% and 80% of the initial ones. Conversely new resonances, attributable to the Al–Cp ethylene insertion product **4**, appeared. After 6 h the molar ratio of **4**:**2** was almost 1:1. ^1H NMR for compound **4**, selected resonances (ClC_6D_5 , 293 K): δ -0.85 (s, 3H, Al-CH₃), 1.07 (s, 3H, B-CH₃), -0.46 (dd, 1H, Al-CHaHb-), -0.26 (Al-CHaHb- (dd, 1 H, Al-CHaHb-), 1.84 (s, 3H, NMeMe'), 1.89 (s, 3H, N-MeMe'), 2.95 (m, 1H, Hd), 5.94 (d, 1H, H Cp), 6.26 (d, 1H, H Cp), 6.47 (s br, 1H, H Cp). ^{19}F NMR (ClC_6D_5 , 293 K): δ -132.2 (d, 3J = 22 Hz), -164.9 (t, 3J = 21 Hz), -167.3 (t, 3J = 21 Hz).

Reaction of $[\text{C}_5\text{H}_5(\text{CH}_2\text{CH}_2\text{NMe}_2)\text{AlMe}]^+[\text{MeB}(\text{C}_6\text{F}_5)_3]^-$ (2**) with Propene.** In a glovebox dimethyl [2-(*N,N*-dimethylethylene)cyclopentadienyl]Al(III) (13 mg, 0.065 mmol) was allowed to react with $\text{B}(\text{C}_6\text{F}_5)_3$ (33 mg, 0.065 mmol) in 0.5 mL of $\text{C}_6\text{D}_5\text{Cl}$ containing C_6H_6 as internal standard (0.08 M) at 23 °C. Propylene was injected by syringe (3 equiv, measured by ^1H NMR). The reaction was monitored via NMR spectroscopy at room temperature, giving the reaction product **3**. Two hours after the addition of propene the amount of species **3** resulted in a 1:2 ratio with respect to species **2**. Species **3** was characterized by ^1H , ^{13}C , DEPT, homonuclear and heteronuclear COSY, and direct and long-range ^1H – ^{13}C correlation NMR experiments. The NMR data are reported in Tables 1, 2, and 3. ^{19}F NMR (ClC_6D_5 , 293 K): δ -132.2 (d, 3J = 22 Hz), -164.9 (t, 3J = 21 Hz), -167.3 (t, 3J = 21 Hz).

A second experiment was performed as above, but after a 2 h period, some of the propene was removed by three freeze–pump–thaw cycles, becoming one-third of the species **2**. The tube was maintained at 23 °C, and the reaction was monitored by ^1H NMR. The NMR spectra, registered every 15 min in a 12 h period, showed that the molar ratio between the species **2**, **3**, and propene was unchanged.

In another experiment, performed as above, after the 2 h reaction time, more propene was added by syringe, replacing that consumed. The tube was kept at 23 °C, and the reaction was monitored by ^1H NMR. The NMR spectra showed that species **2** was gradually converted in species **3**; in a 30 h reaction period species **3** became the prevalent one (in 1.5:1 molar ratio with respect to species **2**).

In a further experiment, performed as above, 2 h after the addition of propene, ethylene was added by syringe and the reaction was monitored by ^1H NMR. After 4 h the concentration of species **3** remained unchanged. On the contrary, the concentration of species **2** decreased, as well as the concentration of ethylene, and resonances attributable to species **4** were detected.

Computational Details

Gas phase electronic structure calculations were carried out using the ADF²⁸ and Gaussian03²⁹ suites of codes, employing both density functional theory (DFT) and post Hartree–Fock *ab initio* methods, the latter at the second-order Møller–Plesset (MP2) level of theory. The DFT calculations employing the ADF program were carried out using the local exchange–correlation potential by Vosko et al.,³⁰ augmented in a self-consistent manner with Becke's exchange-gradient correction³¹ and Perdew's correlation-gradient correction,³² and mostly used to obtain initial geometries for further refinement. Double- ζ Slater-type orbitals (STO) were used for carbon (2s, 2p) and hydrogen (1s), augmented with single 3d and 2p functions (respectively). Aluminum was described using a triple- ζ STO quality basis set augmented with a 4d polarization function. Calculations carried out with the Gaussian suite employed the 6-311+G(d,p) basis set in conjunction with DFT-B3LYP and MP2 models. Mulliken population analysis was carried out using the 6-31G(d) basis set. Geometries for all species (i.e., cation, olefin complexes, transition states (TSs), and final products) were fully optimized using B3LYP/6-311+G(d,p), and the stationary points found were characterized by means of frequency calculations. Structural optimizations of the putative catalytic cationic species **2**

(28) *Amsterdam Density Functional Package*, Release 2000.1; Vrije Universiteit: Amsterdam, 2000.

(29) Frisch, M. J.; Trucks, G. W.; Schlegel, H. B.; Scuseria, G. E.; Robb, M. A.; Cheeseman, J. R.; Montgomery, J. A.; Vreven, T., Jr.; Kudin, K. N.; Burant, J. C.; Millam, J. M.; Iyengar, S. S.; Tomasi, J.; Barone, V.; Mennucci, B.; Cossi, M.; Scalmani, G.; Rega, N.; Petersson, G. A.; Nakatsuji, H.; Hada, M.; Ehara, M.; Toyota, K.; Fukuda, R.; Hasegawa, J.; Ishida, M.; Nakajima, T.; Honda, Y.; Kitao, O.; Nakai, H.; Klene, M.; Li, X.; Knox, J. E.; Hratchian, H. P.; Cross, J. B.; Adamo, C.; Jaramillo, J.; Gomperts, R.; Stratmann, R. E.; Yazyev, O.; Austin, A. J.; Cammi, R.; Pomelli, C.; Ochterski, J. W.; Ayala, P. Y.; Morokuma, K.; Voth, G. A.; Salvador, P.; Dannenberg, J. J.; Zakrzewski, V. G.; Dapprich, S.; Daniels, A. D.; Strain, M. C.; Farkas, O.; Malick, D. K.; Rabuck, A. D.; Raghavachari, K.; Foresman, J. B.; Ortiz, J. V.; Cui, Q.; Baboul, A. G.; Clifford, S.; Cioslowski, J.; Stefanov, B. B.; Liu, G.; Liashenko, A.; Piskorz, P.; Komaromi, I.; Martin, R. L.; Fox, D. J.; Keith, T.; Al-Laham, M. A.; Peng, C. Y.; Nanayakkara, A.; Challacombe, M.; Gill, P. M. W.; Johnson, B.; Chen, W.; Wong, M. W.; Gonzalez, C.; Pople, J. A. *Gaussian 03, Revision B.03*; Gaussian, Inc.: Pittsburgh, PA, 2003.

(30) Vosko, S. H.; Wilk, L.; Nusair, M. *Can. J. Phys.* **1980**, *58*, 1200.

(31) Becke, A. D. *Phys. Rev. A* **1988**, *38*, 3098.

(32) Perdew, J. P. *Phys. Rev. B* **1986**, *33*, 8822.

suggested in Scheme 1 were carried out using two different DFT functionals starting from sensible initial geometries with the aluminum coordinated to the amine group and the Cp ring. Structures for the complex between the cation and ethylene (**CE**) were subsequently optimized adding the olefins in positions favoring the interaction between the vacant coordinative site of Al and the olefin π -bond to the lowest energy structure of the cationic species.

The search for a transition state (TS) describing the insertion of ethylene into the Al–Cp bond (**TS-E1**) was conducted by means of constrained scans along the distance between an ethylene carbon atom and one of carbon atoms in position 3 from the dimethylaminoalkyl group on the Cp ring; putative TS structures were successively refined with a normal TS optimization carried out with the Berny algorithm in conjunction with analytical second derivatives. Geometries for the end product (**PE1**) were obtained relaxing structures having surmounted the energy barrier for the reaction. Similarly, the TS search for the insertion of ethylene into the Al–Me bond (**TS-E2**) was performed by means of a two-step procedure. First, an energy minimization was carried out with the system being constrained to have the distance between the C atom of the Me–Al group and a sp^2 carbon of the olefin at 2.1 Å. The TS geometry was successively refined as indicate above for the insertion into the Al–Cp bond. A similar strategy was used for locating the stationary points on the potential energy surface of the reaction between propene and **2**.

Single-point MP2 calculations using the 6-311+G(d,p) basis set were carried out on the B3LYP/6-311+G(d,p)-optimized structures. NMR chemical shifts for carbon and hydrogen were computed at the B3LYP/6-311+G(2d,2p)//B3LYP/6-311+G(d,p) level of theory in the gas phase with the gauge independent atomic orbitals (GIAO)²² using analytical derivatives.

Acknowledgment. The authors are grateful to Dr. Patrizia Oliva for performing NMR experiments. This work was supported by the Italian Ministry of University and Research (FAR 2007-Università del Sannio).

Supporting Information Available: Additional NMR spectra and Cartesian coordinates for the optimized species are available free of charge via the Internet at <http://pubs.acs.org>.

OM800993E